JCTC Journal of Chemical Theory and Computation

Cation-π Interactions in Serotonin: Conformational, Electronic Distribution, and Energy Decomposition Analysis

Jaturong Pratuangdejkul,[†,‡,#] Pascale Jaudon,[○] Claire Ducrocq,[§] Wichit Nosoongnoen,[†,‡,¥] Georges-Alexandre Guerin,[∥] Marc Conti,[⊥] Sylvain Loric,[£] Jean-Marie Launay,[†,‡] and Philippe Manivet*[,†,‡]

Service de Biochimie et de Biologie Moléculaire, IFR 139, Hôpital Lariboisière, 2, rue Ambroise Paré, 75475 Paris Cedex 10, France, E.A. 3621, Laboratoire de Biologie Cellulaire, UFR des Sciences Pharmaceutiques et Biologiques, 4 Avenue de l'Observatoire, 75270 Paris, Cedex 06, France, I.C.M.M.O. Laboratoire de Chimie Structurale Organique, Université Paris-Sud, Bat. 410, 91405 Orsay, Cedex, France, Institut de Chimie des Substances Naturelles, CNRS, F-91198 Gif-sur-Yvette, France, BioQuanta Corp., 2850 South Parker Road (S) 720, Aurora, Colorado 80014, Service de Biochimie 1, Hôpital Bicêtre, 78, rue du Général Leclerc, 94275 le Kremlin-Bicêtre Cedex, France, 7086, 1 rue Guy de la Brosse, 75005 Paris, France, and Laboratoire de Biochimie-Génétique, Hôpital Henri Mondor, 51, rue du Maréchal de Lattre de Tassigny, 94010 Créteil, France

Received January 25, 2006

Abstract: An adiabatic conformational analysis of serotonin (5-hydroxytryptamine, 5-HT) using quantum chemistry led to six stable conformers that can be either +gauche (**Gp**), -gauche **(Gm**), and anti (**At**) depending upon the value taken by ethylamine side chain and 5-hydroxyl group dihedral angles ϕ_1, ϕ_2, and ϕ_4, respectively. Further vibrational frequency analysis of the **GmGp**, **GmGm**, and **GmAt** conformers with the 5-hydroxyl group in the anti position revealed an additional red-shifted N−H stretch mode band in **GmGp** and **GmGm** that is absent in **GmAt**. This band corresponds to the 5-HT side-chain N−H bond involved in an intramolecular nonbonded interaction with the 5-hydroxy indole ring. The influence of this nonbonded interaction on the electronic distribution was assessed by analysis of the spin−spin coupling constants of **GmGp** and **GmGm** that show a marked increase for C_2-C_3 and C_8-C_9 bonds in **GmGm** and **GmGp**, respectively, with a decrease of their double bond character and an increase of their length. The Atoms in Molecules (AIM), Natural Bond Orbital (NBO), and fluorescence and CD spectra (TDDFT method) analyses confirmed the existence in **GmGp** and **GmGm** of a through-space charge-transfer between the HOMO and the HOMO-1 π-orbital of the indole ring and the LUMO σ^* N−H antibonding orbital of the ammonium group. The strength of the cation-π interaction was determined by calculating binding energies of the NH_4^+/5-hydroxyindole complexes extracted from stable conformers. The energy decomposition analysis indicated that cationic-π interactions in the **GmGp** and **GmGm** conformers are governed by the electrostatic term with significant contributions from polarization and charge transfer. The lower stability of the **GmGm** over the **GmGp** comes from a higher exchange repulsion and a weaker polarization contributions. Our results provide insight into the nature of intramolecular forces that influence the conformational properties of 5-HT.

1. Introduction

Serotonin (5-hydroxytryptamine, 5-HT) belongs to the group of monoamines neurotransmitters that includes catecholamines (dopamine, noradrenaline, adrenaline) and histamine. 5-HT is widely distributed in various organisms and controls a wide variety of physiological and behavioral processes[1]

* Corresponding author e-mail: crcb.manivet@lrb.ap-hop-paris.fr.
† Hôpital Lariboisière.
‡ UFR des Sciences Pharmaceutiques et Biologiques.
§ Institut de Chimie des Substances Naturelles.
∥ BioQuanta Corp.
⊥ Hôpital Bicêtre.
○ Université Paris-Sud.
£ Hôpital Henri Mondor.
On leave from the Department of Microbiology, Faculty of Pharmacy, Mahidol University, 447 Sri-Ayudhaya Rd., Rajtaevee Phayathai, Bangkok 10400, Thailand.
¥ On leave from the Department of Pharmacy, Chaiyaphum Hospital, Chaiyaphum province, Thailand 36000.

10.1021/ct0600316 CCC: $33.50
Published on Web 03/08/2006

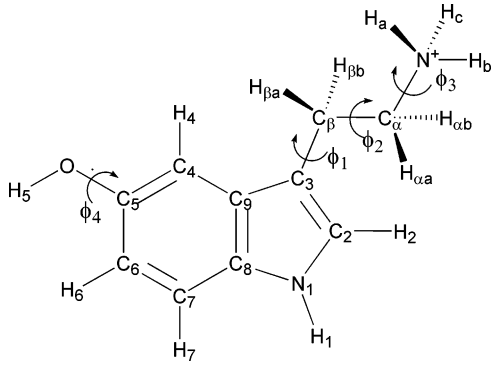

Figure 1. Atomic numbering scheme and definition of dihedral angles of the 5-HT molecule. The four dihedral angles are defined as ϕ_1 ($C_9-C_3-C_\beta-C_\alpha$), ϕ_2 ($C_3-C_\beta-C_\alpha-N$), ϕ_3 ($C_\beta-C_\alpha-N-H_a$), and ϕ_4 ($C_4-C_5-O-H_5$).

mainly through 15 different receptors types.[2] The intensity and duration of 5-HT signaling is determined by its reuptake into cells through the 12 transmembrane domain (TMDs) 5-HT transporter.[3] The important physiological roles of 5-HT and its implications in many pathological states has stimulated intensive research on the design of drugs targeting the serotonergic system. Since drug design needs a clear understanding of the physicochemical properties of the natural compound that is generally used as reference for in silico protocols, it is of prime importance to explore the conformational properties of 5-HT.

At physiological pH, 5-HT is protonated[4] and exists in several conformers due to the flexibility of its ethylamine side chain and the value taken by dihedral angles ϕ_1 and ϕ_2 (see Figure 1 for definitions of ethylamine side-chain dihedral angles). The two 5-HT dihedral angles ϕ_1 and ϕ_2 can be either in +gauche (**Gp**), −gauche (**Gm**), or anti (**At**) conformation, and the 5-HT conformers will be henceforth named in the text as for example **GpAt** when ϕ_1 is in the +gauche conformation and ϕ_2 in the anti conformation. Conformational analysis of 5-HT has been performed using various theoretical calculations and experimental methods. Dating back to the early 1970s, several theoretical calculations have shown the existence of low-energy conformers of 5-HT in the gas phase,[5] and empirical and semiempirical PCILO quantum mechanical calculations suggested that both the **GpGp** and **GpAt** conformers exist in aqueous solution,[6] a fact confirmed by NMR experiments.[7] In the crystalline state, 5-HT exhibits either a **GpGp**, **GpGm**, or **GpAt** conformation depending on the nature of the salt used.[8] Later, based on this information, a mixed model including explicit water solvent without periodic boundary conditions and an empirical force field containing a Coulombic term with a distance-dependent dielectric constant was used to perform molecular dynamics simulations on 5-HT.[9] These simulations showed the existence of the ϕ_1 and ϕ_2 in the **Gp**, **Gm**, and **At** conformations in water, whereas only the **Gp** and **Gm** conformations were observed in the gas phase. A protonated 5-HT conformational analysis has been performed at the B3LYP/6-31G(d) theory level.[10] The authors have reported a set of stable conformers including mirror images and corresponding transition states in the gas phase, with their relative conformational stability in various solvents modeled implicitly by using a polarized continuum model. More recently, gas-phase conformational analysis of protonated 5-HT has been performed at the B3LYP/6-31G(d) up to B3LYP/6-311++G(d,p) theory levels,[11] in aqueous solution using a continuum solvent model. Unfortunately, all the available theoretical studies on 5-HT lack a real description of the nature and amplitude of the intramolecular interactions that influence the conformational stability of 5-HT. The main reason comes from the small basis sets used in the calculations to describe weak nonbonded interactions such as charge transfer, one of the components of cation-π interactions, that need extended basis sets to be correctly described. Since 1971, it is widely admitted that cation-π interactions between indole π-electrons and the cationic head of 5-HT are at the origin of the higher stability of the **GmGp** and the **GmGm** conformers over the **GmAt** conformer.[5b,9] Hence, a non-negligible charge transfer could account mainly for the stabilizing forces in those cation-π interactions. Despite some theoretical calculations of energy decomposition that have been performed on ammonium/pyrole or benzene complexes,[12] until now, no quantum chemistry calculations have been carried out to assert the real existence of such interactions in 5-HT. The goal of the present study was thus to investigate the physicochemical nature of the intramolecular nonbonded forces driving the conformational behavior of 5-HT. For this purpose, we have first studied the whole molecule of 5-HT by performing an adiabatic conformational search in the gasphase in order to find local energy minima and transition-state conformations. The calculated NMR shifts and spin−spin coupling constants of three selected local minima, i.e. **GmGp**, **GmGm**, and **GmAt**, were in good agreement with available NMR experimental data. The calculated IR spectra as well as the topological and natural bond orbital analyses revealed the existence of a real through-space intramolecular charge transfer between the indole π-orbitals and the cationic head N−H antibonding orbital. To further appreciate the relative contribution of this charge transfer in the cation-π interaction with those of other dispersive and nondispersive forces, we performed an energy decomposition analysis on NH_4^+/5-hydroxyindole complexes extracted from the three whole 5-HT local minima optimized geometries.

Our investigations enabled us to provide additional and important insight on the cation-π interactions present in the 5-HT molecule. Furthermore, our results will be useful for the development of accurate force fields for 5-HT, 5-HT derivatives, and 5-HT/5-HT receptor or transporter modeling, that are important for the preparation of new drugs.

2. Computational Methods

An adiabatic conformational analysis of 5-HT was performed by setting the dihedral angle ϕ_1 to 90° and −90° and by rotating ϕ_2 by increments of 60°, while ϕ_3 was left free and ϕ_4 was assigned to 0° or 180° (for definition of dihedral angles, see Figure 1). At each point of the conformational search, the geometry of 5-HT was fully optimized using the DFT-B3LYP method[13] and the 6-31G(d) basis set in the gas phase. All the geometries and energies of stable conformers were further refined by performing a full optimization at the

B3LYP/6-31+G(d,p) theory level, followed by a vibrational frequency analysis in order to verify that each stationary point was a real minimum.

The transition state between two stable conformers was located using the QST3[14] method. The initial guess transition state was obtained from geometry selected along the molecular dynamics (MD) trajectory of 5-HT. Langevin MD simulations were performed in the microcanonical ensemble for 1000 ps. Bond lengths were constrained with the SHAKE algorithm, and the integration time step was 2 fs using the CHARMM molecular mechanics package (see the Supporting Information for details).[15] Finally, vibrational frequency analysis was performed on all optimized transition states in order to reassert their reality.

Infrared (IR) stretch spectra, i.e. wavenumbers (ν) in cm^{-1} and intensities (I) in km/mol, of 5-HT conformers were obtained using vibrational frequencies calculated at the B3LYP/6-31+G(d,p) level. A scaling factor of 0.9605 was applied in order to bring the fundamental stretch of indole N−H into agreement with previously published experimental data.[16]

The NMR isotropic shieldings (σ) were calculated using the Gauge-Including Atomic Orbitals (GIAO)[17] method at the B3LYP/6-311+G(2d,2p) theory level. Calculations were performed on the geometries optimized in the gas phase at the B3LYP/6-31+G(d,p) theory level. The NMR shifts (δ) for 5-HT were calculated using as references tetramethylsilane (TMS) for the C-atom and *tert*-butyl alcohol for the proton. The one-bond NMR spin−spin coupling constants $^1J(A,B)$[18] associated with atoms A and B were also determined.

A topological analysis was performed in order to calculate the charge density (ρ) and its second Laplacian derivative of charge density ($\nabla^2\rho$) for the bond critical points (BCP) using the Bader's Atoms in Molecules (AIM) theory.[19] To evaluate the direction and magnitude of the charge-transfer interactions, the Natural Bond Orbital (NBO)[20] analysis of 5-HT conformers was performed using the NBO 3.1 program.[21] Moreover, the effects of electron delocalization and the vertical excitation energies for the singlet excited states of 5-HT conformers were calculated in the gas phase using the time-dependent density functional theory (TDDFT) method.[22] All calculations were performed using the B3LYP/6-311+G(2d,2p) theory level based on the B3LYP/6-31+G(d,p) optimized geometries.

To get a better understanding on the nature and strength of cation-π interactions, NH_4^+/5-hydroxyindole complexes were generated using geometries of both the 5-hydroxyindole ring and the protonated amine group, which were extracted from whole optimized geometries of 5-HT local energy minima. A hydrogen was added to C_3(sp3) and N(sp3) atoms in order to fill the unsatisfied valence resulting from the broken C_β(sp3)−C_3(sp2) and C_α(sp3)−N(sp3) bonds. Binding energies (BE)[23] of the complexes were refined from single point energy calculations using the HF, B3LYP, and MP2 methods at the 6-311+G(d,p) basis set. The basis set superposition error (BSSE) for each complex was estimated using the full counterpoise method[24] at each level of calculation.

To emphasize the constraints imposed on internal coordinates in 5-HT by intramolecular nonbonded interactions, we fully relaxed and optimized the 5-hydroxyindole ring and the protonated amines group separately at the B3LYP/6-31+G(d,p) theory level. We therefore compared their internal energy within the complexes and after optimization by calculating the 5-HT deformation energy (ΔE_{def}).

Energy of the complexes was decomposed at the HF/6-311+G(d,p) theory level, into physical meaningful terms[25] of individual energetic components using the Kitaura and Morokuma (KM)[26] and reduced variational space self-consistent field (RVS)[27] decomposition analysis.

All quantum mechanics calculations were performed using the Gaussian 03W[28] program package, except for the KM and RVS decomposition analysis which were performed using Gordon and Chen[29] analysis in the GAMESS USA[30] package of programs. All 5-HT structures and molecular orbitals were visualized using the ChemCraft 1.4 beta software.[31] MD simulations were performed using CHARMM 31 running on Silicon Graphics O_2 R12000 workstation under the IRIX 6.5 operating system.

3. Results and Discussion

3.1. Conformational Analysis of 5-HT. 3.1.1. Gas-Phase Adiabatic Conformational Analysis of 5-HT. Potential energy surface (PES) scans are helpful for generating accurate empirical mechanics force field parameters for 5-HT. The adiabatic conformational search performed at the B3LYP/6-31G(d) theory level revealed the existence of six stable conformers of 5-HT and their six mirror images, in good agreement with previously published data.[10,11] Gas-phase energies in Hartrees, the values of 5-HT dihedral angles (ϕ_1, ϕ_2, and ϕ_4), and all the conformers and their relative energies are shown in Figure S1 and Tables S1 and S2 in the Supporting Information. The results show that conformers **1**−**6** and their corresponding mirror image conformers **7**−**12** are redundant since they have the same internal coordinates and relative energies. The results show that dihedral angles ϕ_4 of 5-hydroxyl group in conformers **1**−**3** are in the anti-conformation (OH-anti), while those in conformers **4**−**6** are in the syn-conformation (OH-syn). Depending upon the value of ϕ_2 dihedral angle, with ϕ_1 set in the **Gm** position, 5-HT conformers can be as follows: (i) +gauche (**GmGp**) when it folds on the phenol ring side (conformers **1**, **4**), (ii) −gauche (**GmGm**) when it folds on the pyrole ring side (conformer **2**, **8**), or (iii) anti (**GmAt**) when it extends from the indole ring (conformers **3**, **9**).

Energetically, OH-anti conformers are more stable than the corresponding OH-syn conformers. For OH-anti conformers, the **GmGp** conformer (**1**) is the global minima followed by the **GmGm** conformer (**2**). For OH-syn conformers, **GmGp** and **GmGm** are the next most stable. In the gas phase whatever the position (anti or syn) of the 5-hydroxy group, the lowest energy conformers correspond to the **GmGp** and **GmGm** conformers. However, their difference in energy is not significant. The origin of this stability is due to the stabilizing electrostatic interactions

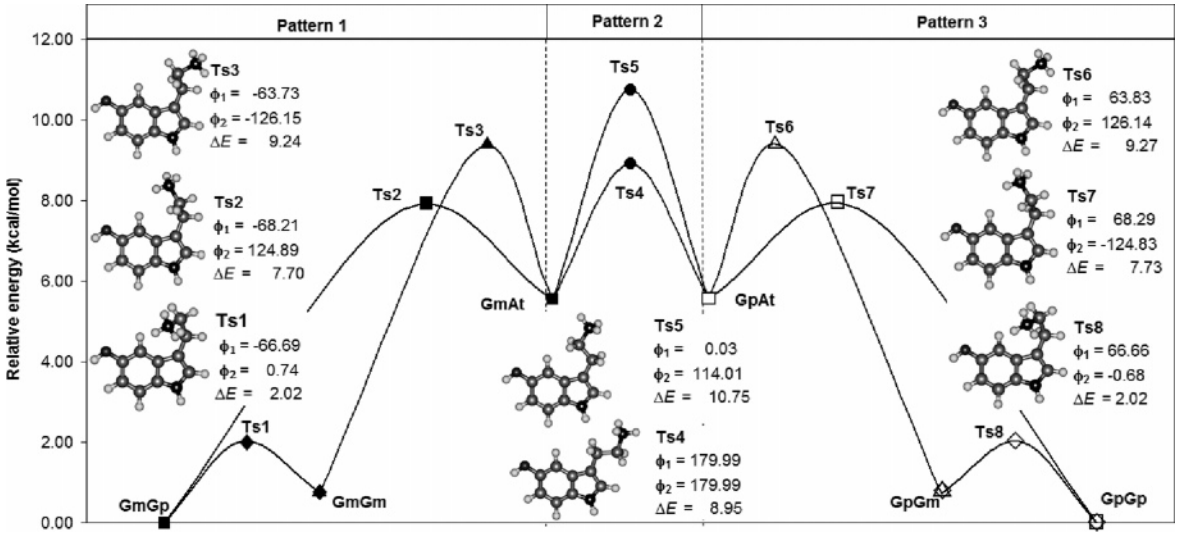

Figure 2. Relative energies (ΔE) in kcal/mol, dihedral angles (ϕ_1 and ϕ_2) in degree of local minima and Ts conformers, and structures of all Ts localized along the interconversion pathway between 5-HT OH-anti local minimum conformations. Calculations were performed using the QST3 Method at the B3LYP/6-31+G(d,p) theory level. Pattern 1 (black squares, triangles, and diamonds) and pattern 3 (white squares, triangles, and diamonds) refer to the two groups of mirror images defined by the value of the ethylamine side-chain dihedral angle ϕ_1. Pattern 2 (black and white circles) refers to the Ts structures between the two groups of mirror images.

occurring between the π-electron cloud of the indole ring and the cationic protonated amine group of 5-HT.

Reoptimization of all the conformers at the B3LYP/6-31+G(d,p) level did not modify significantly their internal coordinates value or their relative energies (see Tables S1 and S2 in the Supporting Information).

3.1.2. Location of Transition States on the 5-HT Potential Energy Surface (PES). To fully scan the PES of 5-HT, to understand the interconversion process of the ethylamine side chain between two neighboring stable conformers and to confirm the existence of the six local energy minima on the PES, we localized the transition-state (Ts) structures using the QST3 method at the B3LYP/6-31+G(d,p) theory level. To save calculation time for this study, only the most stable 5-HT OH-anti conformers and their corresponding mirror images were considered as representative of the entire population of 5-HT conformers. Using the above quantum chemistry PES study in the gas phase, we generated the first set of empirical mechanics parameters that were used to perform MD simulations of 5-HT. Guess conformations for the Ts study using QST3 calculations were extracted from Langevin MD simulation trajectories by a clustering method (additional MD data are provided in the Supporting Information, see Figure S2). The results of QST3 optimization are shown in Figure 2 including structures, dihedral angles, and energy barriers of Ts linking two stable conformers. The analysis of vibrational frequency spectra of Ts structures revealed only one imaginary frequency indicating that all the conformations were real transition states.

In a recent publication,[10] the transition states between two 5-HT minima have been located using the QST3 method. However, the conformers used as the reactant and the product for QST3 calculations were arbitrarily extracted from the 5-HT PES, without any respect for the reliability of the dynamics of the interconversion process of the ethylamine side chain. For instance, an **GmAt**-like conformer was found as a transition state between two conformers belonging to a different group of mirror images (conformers **2** and **8** in the present work). In our strategy we avoided bias in the choice of guess transition-state conformers for QST3 calculations. This was achieved by selecting adequately reactant and product conformers, based on the analysis of authorized rotation of the ethylamine side-chain dihedral angles along MD trajectories. This strategy requires a good set of empirical molecular mechanics force field parameters. We generated the first set of CHARMM parameters based on the adiabatic conformational analysis (Table S1 in the Supporting Information) performed at the B3LYP/6-31+G(d,p) level and used MD simulations to obtain guess transition-state conformers for the QST3 calculations. Finally, the transition states located using the QST3 method were used to refine the first set of CHARMM parameters and to confirm the reliability of the transition-state conformers. Only one imaginary frequency was found in vibrational frequency analysis for all optimized structures, confirming they are real transition states with a first-order saddle point. Visual inspection of the vectors of the atomic motions for the negative imaginary frequency along the reaction coordinates enabled us to check that the geometry of transition states corresponded to motions required for the mechanistic scheme.

Figure 2 shows that **pattern 1** and **pattern 3** are symmetric since they have the same energy barriers and symmetric geometries (dihedral angles in opposite signs), **Ts1**, **Ts2**, and **Ts3** being symmetric with **Ts8**, **Ts7**, and **Ts6**, respectively. In **pattern 1**, ethylamine side-chain interconversion between conformers **GmGp**, **GmGm**, and **GmAt** passes through transition states where the dihedral angle ϕ_2 is mostly driving the conformational changes. The dihedral angle ϕ_1 undergoes changes imposed by dihedral angle ϕ_2 in order to accommodate the conformation to the intramolecular nonbonded interactions. For **Ts1** and **Ts2**, dihedral angles ϕ_1 are similar.

Figure 3. Structures of the three most stable 5-HT conformers **1**, **2**, and **3** (**GmGp**, **GmGm**, and **GmAt**, respectively). 5-OH groups in anti position.

In **Ts3**, the attraction between the cationic head and the π-electrons of the five-membered ring constrains the dihedral angle ϕ_1 to accommodate to a value of $-63.73°$ to finally get the value of $-64.40°$ when **Ts3** evolves toward the **GmGm** conformer (conformer **2**). Those results, interpreted with the above observation of a higher stability of **GmGp** conformers compared to **GmGm**, suggest that the most important constraints imposed on 5-HT internal coordinates concern **GmGm** conformers. However, the relative energy between **GmGp** and **GmGm** conformers is very small. This reinforces the hypothesis of an existing balance in **GmGm** conformers between stabilizing intramolecular electrostatic interactions between the cationic head and π-electrons of the five-membered ring and strong destabilizing repulsive interactions.

The high relative energy of **Ts3** might be attributed to a progressive loss of stabilizing nonbonded interactions between the cationic head and π-electrons of the indole ring upon rotation of the ethylamine side chain from **GmGm** to **GmAt** conformers. These nonbonded interactions could be sufficient to attract the cationic head and maintain the stability of **Ts3** but too weak to balance the internal coordinate constraints imposed on ϕ_1. Surprisingly, the energy barrier between **GmGm** and **GmGp** is not high (2 kcal/mol) suggesting that interconversion between **GmGp** and **GmGm** conformers is relatively easy by rotation of the ethylamine side chain above the 5-HT ring plane. The largest constraints imposed by steric hindrance on internal coordinates in **Ts1** are bending angles θ_1 and θ_2 that are opened about 3° compared to **GmGp** and **GmGm** conformers (5° and 2° for the **GmAt** conformer θ_1 and θ_2 angles, respectively). The ethylamine side chain accommodates the repulsion upon rotation above the indole ring plane by opening θ_1 and θ_2 angles. During MD simulations, interconversion of the side chain between two groups of mirror images of **patterns 1** and **3** occurs only between **GmAt** and **GpAt**, through **Ts4** and **Ts5**. For **Ts4** and **Ts5** dihedral angle ϕ_1 the value is 0° or 180°, respectively, whereas the dihedral angle ϕ_2 is in anti orientation for both transition states.

3.2. Physicochemical Analysis of 5-HT. To better understand the nature of driving forces that influence the conformational properties of 5-HT, we further investigated the nature of intramolecular interactions and their relative weight in 5-HT. For this purpose, we have focused our attention on the three stable conformers **1**, **2**, and **3** (**GmGp**, **GmGm**, and **GmAt**, respectively) in which the ethylamine side chain is on the same side of the indole ring and 5-OH groups in the anti position (Figure 3 and Tables S2 and S3 in the Supporting Information).

3.2.1. Calculated Infrared (IR) Spectra of 5-HT. Harmonic vibrational frequencies (ν) and IR intensities (I) of three representative conformers (Figure 3) were calculated at the B3LYP/6-31+G(d,p) level. A scaling factor of 0.9605 was applied to frequencies of 5-HT conformers in order to bring the fundamental indole NH stretches into agreement with experimental results of the indole molecule (3525 cm^{-1}).[16a] This sharp band is characteristic of indole derivatives and commonly used for identification of tryptamine and tryptophan derivatives.[16b,32] Seventy-two normal vibrational modes were recorded for the three conformers. However, only frequencies above 2800 cm^{-1} corresponding to the fundamental vibration of stretch modes were analyzed in our study. The stretching modes can be divided into three groups: the heterocyclic system of the indole ring (aromatic CH and indole NH stretches), the ethylamine side chain (alkyl CH and amine NH stretches), and a hydroxyl group (OH stretch). All stretching frequencies and intensities of three 5-HT conformers are listed in Table S4 in the Supporting Information. IR-stretching bands are provided in the Supporting Information in Figure S3.

For the three conformers, the frequencies in the 2800−3050 cm^{-1} region belong to alkyl CH stretches of the ethylamine side chain. The lower frequencies in the 2881−2923 cm^{-1} and the 2985−2979 cm^{-1} regions were characterized as symmetric stretches of $CH_2(\beta)$ and $CH_2(\alpha)$groups, respectively. In addition, frequencies in the 2946−2971 cm^{-1} and the higher-frequency 3048−3035 cm^{-1} regions were identified as antisymmetric stretches of $CH_2(\beta)$ and $CH_2(\alpha)$ groups, respectively. The $CH_2(\beta)$ stretches of the **GmGp** and **GmGm** conformers are quite similar and have higher frequencies and lower intensities than those found for the **GmAt** conformer. The $CH_2(\alpha)$ stretches are similar for the **GmGm** and **GmAt** conformers and have higher frequencies and lower intensities than those of the **GmGp** conformer. The vibrational frequencies in the 3050−3130 cm^{-1} region are attributed to the aromatic CH stretches of the indole ring (3050−3080 cm^{-1} region for the phenyl ring and 3125−3131 cm^{-1} region for the pyrole ring) and are similar for the three conformers.

The alkyl CH stretch frequencies have been claimed to be sensitive to conformational changes in various indole derivatives including the neutral form of 5-HT,[32,33] containing a neutral ethylamine side chain through the interaction of the CH_2 group with the lone pair of amino nitrogen. In the

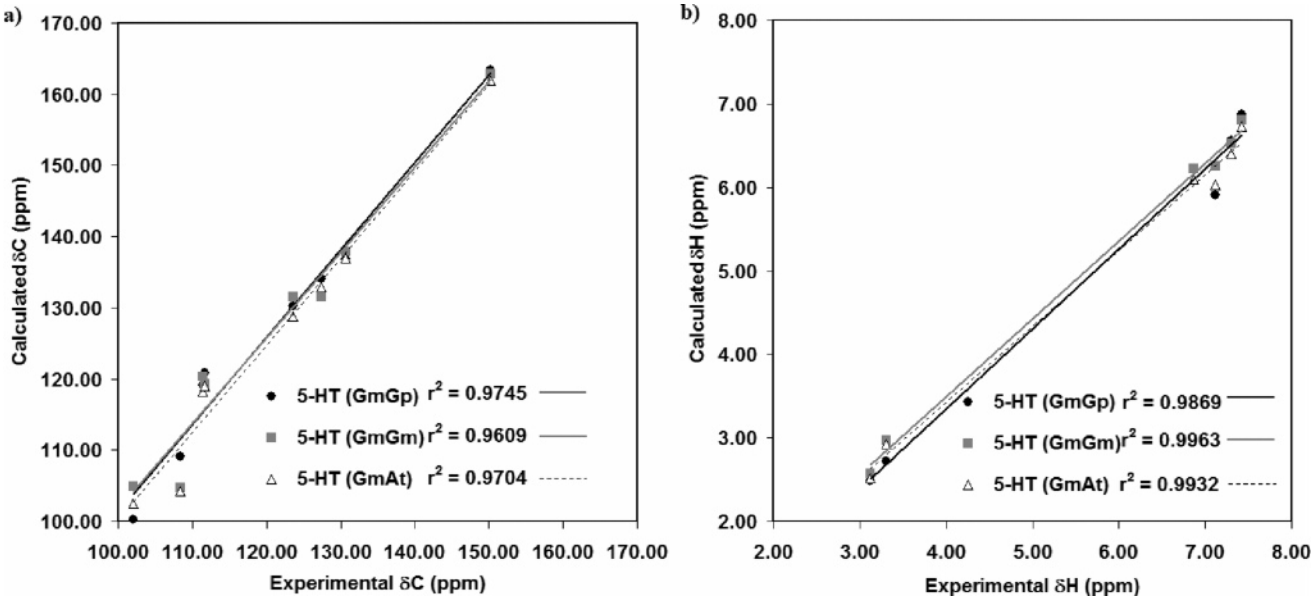

Figure 4. Correlation plots of (a) carbon chemical shift (δC) and (b) H chemical shift (δH) between available experimental and predicted values (Table 1) obtained from the GIAO calculation at the B3LYP/6-311+G(2d,2p) theory level for the three most stable conformers (OH anti, **GmGp**, **GmGm**, **GmAt**).

cationic form of 5-HT, the observed red-shift of $CH_2(\beta)$ stretch frequencies of the **GmGm** and **GmGp** conformers as compared to **GmAt** comes from a phenomenon involving electron transfer from indole π orbital to the CH antibonding orbital of the $CH_2(\beta)$ group. This is confirmed by NBO analysis (see below). The $CH_2(\alpha)$ group is not affected by π electron clouds since it is far away from the indole ring.

Particularities were observed for the three 5-HT conformers in the NH stretch region (3100−3530 cm^{-1}). All 5-HT conformers have four NH stretches: one indole NH stretch and three amine NH stretches. Amine NH stretch frequencies corresponding to the NH bond pointing toward the indole ring of **GmGp** and **GmGm** conformers are strongly red-shifted as compared to that of the **GmAt** conformer, by respectively 114 and 164 cm^{-1}. Hence, very high intensities of those bands were observed in **GmGp** and **GmGm** conformers. In the **GmAt** conformer, no N−H bond is pointing toward the indole ring, and the symmetric vibrational frequency of the three N−H bonds are similar. Two amine NH stretches were identified as antisymmetric stretches. The first antisymmetric NH stretch of **GmGp** and **GmGm** conformers is red-shifted at 3321 cm^{-1} with a higher intensity as compared to the **GmAt** conformer (3358 cm^{-1}). The last antisymmetric NH stretches of **GmGp** and **GmGm** were located in a similar region of frequencies (3377 and 3382 cm^{-1}, respectively), with a blue-shift as compared to the corresponding NH stretch of **GmAt** (3358 cm^{-1}) and a similar intensity. The indole NH and OH stretching modes of the three conformers are located in the 3523 ± 5 cm^{-1} and 3674 ± 3 cm^{-1} regions, respectively, with similar intensities. For amine NH stretches, the relevant red-shifts of harmonic vibrational frequencies and their increase in intensity for **GmGp** and **GmGm** conformers favor the existence of through-space NH-π/indole nonbonded interactions. In the **GmGp** and **GmGm** conformers, the amine $N-H_a$ bond, which points toward the indole ring, is involved in a charge transfer with the indole π-electrons cloud. This is supported by the existence of several physical criteria that are used to appreciate whether a hydrogen bond is established between a hydrogen bond donor and a lone pair of a hydrogen bond acceptor:[16b,34] (i) the elongation of the N−H bond due to the increase of the electron population of the N−H σ^* orbital, (ii) a red-shift of the N−H frequency with enhanced intensity, and (iii) the presence of a bond critical point in the vicinity of the hydrogen bond that we will detail below.

3.2.2. Calculated NMR Isotropic Shielding and Spin−Spin Coupling Constants of 5-HT Conformers. The correlation plots of NMR shifts (Figure 4) show a good agreement between the calculated and the experimental values of carbon chemical shifts δC,[35] for the three conformers. We also evaluated the root-mean-square (rms) deviation of predicted values from experimental ones for each atomic position (Table 1). The largest deviation of calculated δC for the three 5-HT conformers were observed for carbon C_5 (rms deviation of 12 ppm). Although the calculated δC were overestimated, their amplitudes at each position were quite similar to the experimental ones. The calculated H chemical shifts δH of H_2, H_4, H_6, H_7 and the two average values of the side chain H_α and H_β of the three conformers are also in good agreement with experimental data.[35] The three conformers show low rms deviation from predicted values (0.5−0.8 ppm) at each position, except at proton H4 for which rms deviation is 1.08 ppm.

The analysis of calculated NMR isotropic shieldings (σ) revealed that their values change depending upon the conformation adopted by 5-HT (Table S5 in Supporting Information). This is due to a change in the electron density of some atoms in the conformers (see Table S6 in the Supporting Information). This electron redistribution is promoted by the formation of intramolecular interactions between the $N-H_a$ bond of the ethylamine side chain and

Table 1. Experimental and Calculated B3LYP/6-311+G(2d,2p) GIAO δC and δH for the Three Most Stable 5-HT Conformers (OH Anti, **GmGp**, **GmGm**, **GmAt**)

position	exp.	GmGp	GmGm	GmAt	rms
		C-Chemical Shift (δC)			
C_2	123.61	130.29	131.58	128.79	6.71
C_3	108.38	109.06	104.76	104.24	3.20
C_4	101.97	100.24	104.95	102.24	2.00
C_5	150.26	163.36	162.86	161.39	12.31
C_6	111.39	119.17	120.29	118.32	7.91
C_7	111.72	120.92	119.30	118.84	8.02
C_8	130.73	136.82	137.96	137.62	6.75
C_9	127.39	134.09	131.52	132.97	5.57
		H-Chemical Shift (δH)			
H_2	7.30	6.56	6.52	6.35	0.83
H_4	7.12	5.91	6.25	5.99	1.08
H_6	6.87	6.21	6.22	6.13	0.68
H_7	7.42	6.87	6.80	6.65	0.65
H_β(average)	3.12	2.57	2.63	2.52	0.55
H_α(average)	3.31	2.72	2.97	2.94	0.45

the indole ring orbitals. The charge density (calculated with the help of the CHelpG Scheme[36] modifications) concerns mainly carbon atoms C_2, C_3, C_4, C_8, and C_9. In the **GmGm** and **GmGp** conformers, the N−H_a bond points toward C_8−C_9 and C_2−C_3 bonds, respectively, resulting in a withdrawal of electron density located at those bonds. The total potential derived charge of the C_8−C_9 bond (charge C_8 + charge C_9) decreases from 0.23, through 0.28 to 0.32 e^- when 5-HT adopts the **GmGm**, **GmAt**, and **GmGp** conformations, respectively. This effect is most marked on carbon C_9 (from 0.09, through 0.11 to 0.21 e^-). The decreasing electronegativity at carbon C_9 for the **GmGp** conformer and the redistribution of π orbital electrons upon intramolecular interactions led to the decrease of the calculated NMR shieldings $\sigma(C_9)$ that shifted by 1.2 and 2.8 ppm compared to the **GmAt** and **GmGm** conformers. The carbon C_8 charge increases from 0.18, through 0.14 to 0.11 e^- when 5-HT adopts the **GmAt**, **GmGm**, and **GmGp** conformations, respectively, while the **GmGp** calculated NMR shieldings $\sigma(C_8)$ shift by 1.3 and 0.8 ppm in the **GmGm** and **GmAt** conformers, respectively. The total bond charge of the C_2−C_3 bond decreases from −0.24, through −0.20, to −0.14 e^- when 5-HT adopts the **GmGp**, **GmAt**, and **GmGm** conformations, respectively. This effect is not particularly predominant at carbon C_2 or C_3 and the correlation between charge decreases and calculated NMR shieldings is more difficult to establish since electron delocalization and redistribution mitigates the influence of N−H_a. Carbon C_3 undergoes the influence of ethylamine side chain and the decrease of charge (from −0.16, through −0.12, to −0.04 e^- when 5-HT adopts the **GmGp**, **GmAt**, and **GmGm** conformation, respectively), is accompanied by a decrease of the **GmGm** conformer calculated NMR shieldings $\sigma(C_3)$ that shifted by 0.5 ppm compared to the **GmAt** conformer and an increase of $\sigma(C_3)$ that shifted by 5.3 ppm compared to the **GmGp** conformer. This lack of correlation between charges and NMR-carbon shifts $\delta(C_3)$ could be attributed to a greater deviation of the calculated shieldings from the experimental ones. Indeed, Table 1 shows that the greatest deviation between experimental and calculated shifts concerns $\delta(C_3)$.

An additional atomic center of interest is represented by C_4. Carbon C_4 undergoes a change in the natural charge from −0.38, through −0.39, to −0.44 e^- when 5-HT adopts the **GmAt**, **GmGm**, and **GmGp** conformations, respectively. A decrease of the **GmGp** conformer calculated NMR shielding $\sigma(C_4)$ shifts by 2.2 and 4.5 ppm in the **GmAt** and **GmGm** conformers, respectively.

For protons, the most significant modifications of NMR isotropic shieldings upon 5-HT conformational changes are observed for the amine proton H_a in gauche conformers where the N−H_a bond interacts with the indole ring π orbital (Table S5 in the Supporting Information). In those conformers, the proton H_a is localized within the diamagnetic deshielding zone of the six- and the five-membered rings for the **GmGp** and **GmGm** conformers, respectively. As a result, chemical shifts of H_a in the the **GmGm** and **GmGp** conformers are upfield (decrease of $\sigma(H_a)$) with respect to its shift in the **GmAt** conformer and to the shifts of the two other protons of the amine side chain H_b and H_c. To support this we calculated the shielding increment, $\Delta\delta$H, for proton H_a in the **GmGm** and **GmGp** conformers by subtracting H isotropic shielding calculated for optimized ammonium molecule alone to the corresponding H isotropic shielding in the whole 5-HT molecule at the same level of theory (Table S7 in the Supporting Information). An increase of the shielding increment, $\Delta\delta$H, for H_a confirmed the deshielding of the proton in the presence of the π orbitals in 5-HT. An additional deshielding effect on proton H_a is due to the electronegativity of the cationic head nitrogen atom that decreases the electronic density around the proton H_a. This phenomenon is due to the strong polarization of the N−H_a bond when it points either to the C_2−C_3 or to the C_8−C_9 bond in the **GmGm** or the **GmGp** conformer, respectively. We will demonstrate this polarization below, using the energy decomposition analysis.

The observation of calculated one-bond nuclear spin−spin coupling constants (^1J) of 5-HT shows a decrease of the ^1J upon conformational change from the **GmAt** to the **GmGp** and **GmGm** conformers. This is indicated in Table 2 that shows significant differences of calculated ^1J for C_2−C_3, C_3−C_9, C_4−C_9, and C_8−C_9 bonds and modification of their length. If the **At** conformer is used as a reference for internal coordinates, we can show for C_2−C_3, C_3−C_9, and C_4−C_9 bonds an elongation by 0.0018, 0.0024, 0.0041, and 0.0058 Å for the **GmGp** conformer and a bond length increase by 0.0059, 0.0055, and 0.0012 Å for the **GmGm** conformer. As compared to the **GmAt** conformer, calculated $^1J(C_2,C_3)$, $^1J(C_3,C_9)$, and $^1J(C_4,C_9)$ decreased by (i) 2.3, 3.5, and 2.4 Hz and (ii) 4.7, 2.7, and 0.8 Hz for the **GmGp** and **GmGm** conformers, respectively. The decrease of $^1J(C_2,C_3)$, $^1J(C_3,C_9)$, and $^1J(C_9,C_4)$ coupling constants in the **GmGp** and **GmGm** conformers is mainly due to a decrease of their FC contribution (diamagnetic spin−orbit (DSO), paramagnetic spin−orbit (PSO). Fermi contact (FC) and spin dipolar (SD) contributions of $^1J(C_2,C_3)$, $^1J(C_3,C_9)$, and $^1J(C_4,C_9)$ are provided in Table S8 in the Supporting Information). Since

Table 2. Spin−Spin Coupling Constants ^1J(A,B) in Hz of Atoms in 5-Hydroxyindole Ring Using GIAO Method at the B3LYP/6-311+G(2d,2p) Level and Bond Distance in Å (Differ from Bonds in At)

	^1J(A,B)			bond distance		
bond	**Gp**	**Gm**	**At**	**Gp**	**Gm**	**At**
N_1-C_2	10.3	10.4	10.6	−0.0001	−0.0014	1.3713
C_2-C_3	75.1	72.7	77.4	0.0018	0.0059	1.3805
C_3-C_9	53.8	54.6	57.3	0.0041	0.0055	1.4425
C_8-C_9	57.5	57.8	58.0	0.0024	0.0008	1.4192
N_1-C_8	11.0	10.6	10.8	−0.0027	0.0005	1.3870
C_4-C_9	65.8	67.4	68.2	0.0058	0.0012	1.4068
C_4-C_5	77.4	77.1	77.8	0.0016	0.0006	1.3909
C_5-C_6	66.4	66.2	67.0	0.0006	0.0011	1.4140
C_6-C_7	65.8	65.9	66.1	−0.0004	−0.0010	1.3900
C_7-C_8	70.5	70.4	71.0	0.0005	0.0005	1.3980
C_5-O	24.3	24.4	24.2	−0.0032	−0.0034	1.3696
$N-H_a$	50.47	49.43	50.55	0.0097	0.0130	1.0258
$N-H_b$	50.17	51.45	50.09	−0.0007	−0.0017	1.0254
$N-H_c$	50.39	50.17	50.46	−0.0017	−0.0012	1.0256

the FC operator[18] probes the s-electrons at the sites of coupling nuclei, the decrease of the FC contribution of these ^1J coupling constants infers a decreasing s-character of the σ orbital of C_2-C_3, C_3-C_9, and C_4-C_9 bonds. We have also noted a decrease of the SD contribution of the multiple bonds, indicating a decrease of the π-character leading to a weakening of the bonds.[37] However this decrease is more marked for some bonds, depending on the conformation adopted by 5-HT, **GmGp** or **GmGm**. For instance, concerning the **GmGm** conformer, the SD contribution decreased dramatically for the C_2-C_3 bond and to a lesser extent for the C_3-C_9 bond, since the $N-H_a$ bond points to C_2-C_3. For the **GmGp** conformer, the SD contribution decreased for the C_4-C_9 bond. This is consistent with our above observations on electron redistribution, isotropic NMR shielding, and FC contributions. All of these observations favor the existence of a plausible cation-π interactions between $N-H_a$ and the indole ring orbitals where a charge transfer from the π orbital of the 5-hydroxyindole ring to the protonated amine group could occur. In turn, this should affect the conjugated double bond in the indole ring, modifying their bond character. In the **GmGp** conformer we note a decrease of the s-character of the C_8-C_9 bond σ orbital that accounts for the decrease of the FC contribution to the $^1J(C_8,C_9)$ coupling. We also note a decrease of the SD contribution, indicating a weakening of the C_8-C_9 bond. Surprisingly, the value of $^1J(C_8,C_9)$ remains quite constant for the three conformers. The calculated SD and PSO contributions of $^1J(C_8,C_9)$ change (decrease of SD and increase of PSO) as compared to the **GmGm** and **GmAt** conformers, reflecting the change in bond multiplicity. Since the variation of the SD and PSO contribution of $^1J(C_8,C_9)$ compensate each other and the FC contribution change remains subtle, $^1J(C_8,C_9)$ is only weakly different among the three conformers.

3.2.3. Topological Analysis of the Electronic Density. To characterize the formation of intramolecular hydrogen bonds in 5-HT conformers, the topological analysis of the electron density using the "atoms in molecules" (AIM) theory was applied.[38] We used this method to detect bond paths inside the 5-HT molecule and critical points associated with them. Two main kinds of parameters are provided by AIM analysis: the charge densities (ρ) and the corresponding density laplacians ($\nabla^2\rho$) at the bond critical points (BCPs). The value of the electronic density at the BCP for a given bond, $\rho(r_c)$, can be correlated to the concept of bond order[38] with higher values of $\rho(r_c)$ corresponding to stronger bonds. The positive sign of the Laplacian of the charge density at the BCP, $\nabla^2\rho(r_c)$, corresponds to a closed shell interaction that is responsible for the bonding[38] where the electronic charge is concentrated around each nucleus. This is the typical case for ionic or hydrogen bonds. For 5-HT conformers, the existence of a hydrogen bond between the $N-H_a$ bond and the π orbital of the indole ring was confirmed by the presence of BCPs linking amine H_a and indole C_9 ($\rho(r_c) = 0.011564$, $\nabla^2\rho(r_c) = 0.05566$) or C_3 ($\rho(r_c) = 0.019181$, $\nabla^2\rho(r_c) = 0.06119$) atom respectively in conformers **GmGp** and **GmGm**. Our results are in reasonable agreement with the Popolier et al.[38b] criteria used to characterize a D−H···A type hydrogen bond, where D and A are hydrogen bond donor and acceptor atoms, respectively, even if the values of charge density at BCP $\rho(r_c)$ for the **GmGp** and **GmGm** conformers are relatively low compared to the values obtained with strong hydrogen bonded systems with canonical hydrogen bonds. The Popelier et al. criteria also include an increasing charge of the hydrogen atom involved in the hydrogen bond. In our results, the charge of H_a atom of gauche conformers increases as compared to the **GmAt** conformer. We note also for the **GmGm** conformers a higher electron density at the bond critical point as compared to **GmGp.** This is in good agreement with the above observations that suggest the presence of a stronger hydrogen bond in **GmGm**, shown by a more red-shifted and more intense band of N−Ha stretch vibration. Hence, the interatomic distances between H_a and C9 or C3 show that the hydrogen bond is weaker for the **GmGp** ($H_a\cdots C_9 = 2.36$ Å) conformer than for the **GmGm** ($H_a\cdots C_3 = 2.26$ Å) one. All of the above observations confirm the existence of an intramolecular hydrogen bond particularly in the **GmGm** conformer but also in the **GmGp** conformer. The geometrical constraints imposed on the internal coordinates of the ethylamine side chain in the **GmGm** and **GmGp** conformers prevent the formation of an ideal hydrogen bond that is known to have strong anisotropic characteristics. Indeed, it has been shown that the position of the ammonium cation in interaction with the benzene ring in the most stable cation-π complex is bidendate, with two hydrogen atoms pointing toward the benzene ring to form an ideal hydrogen bond.[39] In the **GmGp** and **GmGm** conformers, the position of the cationic head are largely shifted from the centroid of the six- and five-membered rings for the **GmGp** and **GmGm** conformers, respectively. However, in the **GmGm** conformer the cationic head seems to be in a better spatial configuration for the formation of a hydrogen bond than in the **GmGp** one, with a more important overlap of the π_{indole} and σ^*_{N-H} orbitals. We also observed the existence, for the **GmGm** conformer, of a ring critical point between the π_{indole} orbital

Table 3. NBO Analysis of NH-π Indole Remote Contacts in the 5-HT Conformers Calculated Using the B3LYP/6-311+G(2d,2p) Level of Theory

charge-transfer orbital		
donor$_{(i)}$/occupancy (e)	acceptor$_{(i)}$/occupancy (e)	$E^{(2)}$ (kcal/mol)
GmGp		
$\pi(C_8-C_9)$/1.60344	$\sigma^*(N-H_a)$/0.02012	0.56
GmGm		
$\pi(C_2-C_3)$/1.84178	$\sigma^*(N-H_a)$/0.02797	2.80
$\sigma(N-H_a)$/1.99267	$\pi^*(C_2-C_3)$/0.36524	0.56

and the $N-H_a$ bond, confirming a strong through-space cation-π interaction.

3.2.4. Analysis of Electron Distribution in the Ground and Excited States of 5-HT. Since we suspected the presence of a charge transfer between the $N-H_a$ bond and π orbitals of the indole ring, we further studied electron delocalization and their strength by performing the Natural Bond Orbital (NBO) analysis on the ground state of 5-HT. Electron delocalizations were assessed by the estimation of the occupation number and their magnitude determined from an analysis of the off-diagonal elements in the Fock matrix in the NBO basis, taking into account all of the possible donor−acceptor interactions and then calculating the strength of all of them according to second-order perturbation theory, ($E^{(2)}$) (Table 3). The schematic representation of energy levels and contour plots of important molecular orbitals (MOs) in the electronic structures are presented in Figure 5. The results of NBO analysis for the three most stable 5-HT conformers clearly show that the σ^*_{N-Ha} antibonding orbital occupation number in the amine group of the **GmGp** and **GmGm** conformers is strong, suggesting that this orbital is involved in the **GmGp** and **GmGm** conformers in a charge-transfer process, thereby leading to the elongation of the $N-H_a$ bond length, followed by a downshift of stretching vibrational frequency. The two other antibonding orbitals σ^*_{N-Hb} and σ^*_{N-Hc} of the **GmGp** and **GmGm** conformers and the three σ^*_{N-H} orbitals of the **GmAt** conformer have a lower occupation number indicating that they are not involved in any charge transfer. A very strong charge transfer from the π_{C2-C3} orbital to the σ^*_{N-Ha} antibonding orbital is found for the **GmGm** conformer with a stabilization energy $E^{(2)}$ of 2.80 kcal/mol. Hence, a backward direction charge transfer was also found from the donor σ_{N-Ha} orbital to the acceptor π^*_{C2-C3} with a stabilization energy $E^{(2)}$ of 0.56 kcal/mol. A less important, but non-negligible, charge transfer from the π_{C8-C9} orbital to the σ^*_{N-Ha} antibonding orbital was shown for the **GmGp** conformer with a stabilization energy $E^{(2)}$ of 0.56 kcal/mol. Second-order properties, such as the NMR spin−spin coupling constant, can be used together with HOMO-n and LUMO+n gap (HLG) energy to interpret simply the electronic redistribution. The inverse of the energy gap directly enters into the general expression for the coupling constant.[40] The smaller the HLG energy, the larger the spin−spin coupling constants are expected to be. If HLG is taken as a rough estimate of these trends, we can see in Table 2 that the trend for ^1J in the three conformers follow the inverse of HLG. The increase of HLG found for the **GmGp** and **GmGm** conformers as compared to the **GmAt** conformer is due to stabilization of the highest occupied orbitals labeled 46 and 47 (HOMO-1 and HOMO) which are mainly indole ring π orbitals. The increase of the average C−C distances of the indole ring weakens the antibonding character, increases the electronic density at the atomic centers, and thus stabilizes the orbitals. The value of ^1J(C4,C9) and ^1J(C2,C3) for the **GmGp** and **GmGm** conformers respectively are smaller than for the **GmAt** conformer and inversely correlated with HLG. For ^1J(C8,C9) the inverse correlation with HLG is less marked since, as mentioned above, this bond undergoes many electron rearrangements, where SD and PSO contribution compensate and where the density of HOMO and HOMO-1 orbital electrons is high, those orbitals mixing together under perturbations from the nuclear spins.

To further study the electronic structure of 5-HT conformers and rationalize spectroscopic properties of 5-HT, we analyzed the vertical excitation energies of the six low-lying singlet excited states calculated at the optimized geometry of the ground state by using the TDDFT.

The major composition of MOs, the ground states orbital HLG, vertical excitation energies (ΔE) are listed in Table 4. We also reported calculated wavelengths (λ) and oscillator strengths for each state of the three conformers in order to fit with the available experimental spectra. The experimental fluorescence spectra of 5-HT have shown a maximum emission at 336 nm in a wide pH range from 2 to 10 in aqueous solution.[41] This band shifts to 350 nm at pH 12.5 and to 380 nm with a very low quantum yield upon laser excitation at higher pH. The 336, 350, and 380 nm emissions have been assigned to protonated and singly and doubly deprotonated 5-HT, respectively. As shown in Table 4, the first singlet excited state (1^1A) of the **GmGp** conformer corresponds to a calculated wavelength of 336.77 nm, which fits almost perfectly to the emission spectra of 336 nm. Thus, our result strongly confirms this assignment to the cationic form of 5-HT. It is interesting to note that the maximum peak of 5-HT at neutral pH (336 nm) is blue-shifted as compared to that of tryptophan (350 nm) and tryptamine (356 nm), which could be attributed to the hydroxyl group in 5-HT. Those longer wavelength emissions (around 350 nm) have been assigned to the indole-NH_3^+ group interaction.[41] The red-shift of emission at high pH of these molecules has been previously proposed to be due to reduced electrostatic repulsion between the NH_3^+ group and the indole ring.[42] These experimental results provide a satisfactory explanation for the electronic excitation of the **GmGp** conformer. The 1^1A excited state of the **GmGm** conformer presents a calculated wavelength of 357.58 nm (Table 4 and Table S9 in the Supporting Information), which is close to that of tryptamine and to a lesser extent to that of tryptophan. This indicates that the indole-NH_3^+ group interaction is stronger in the **GmGm** conformer than that in the **GmGp** one. Our results can be used to confirm the presence of a charge-transfer between the cationic head of 5-HT and indole π orbitals, shown by the NBO analysis a stronger stabilization energy for **GmGm** than that for **GmGp**. No band could be observed for **GmAt** using the TDDFT calculation, indicating

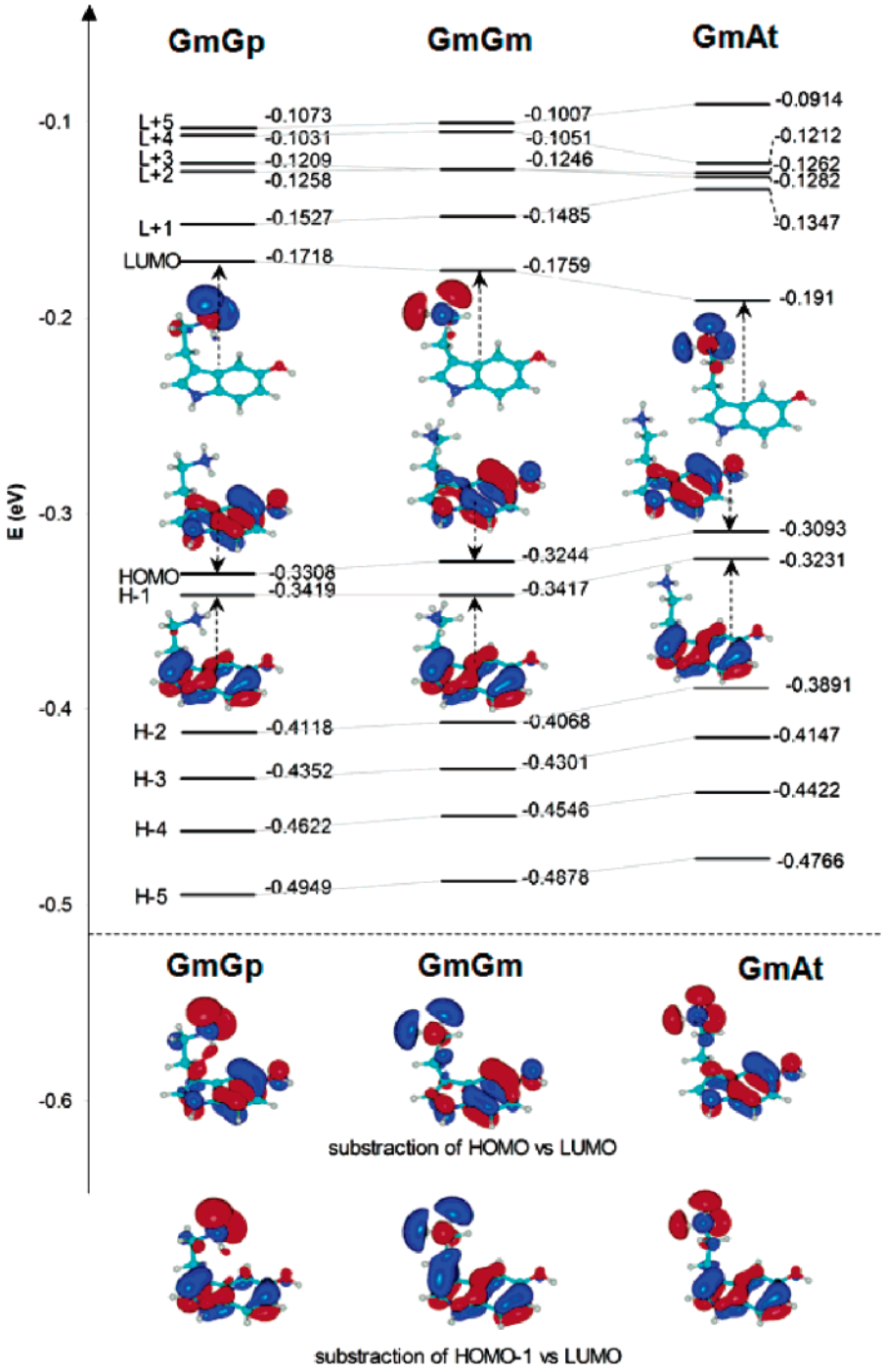

Figure 5. Energy levels (eV) of the 5-HT conformers (**GmGp**, **GmGm**, and **GmAt**) at ground-state calculated using population analysis in gas phase at the B3LYP/6-311+G(2d,2p) level of theory. The HOMO, HOMO-1, LUMO, and the density difference between HOMO vs LUMO and HOMO-1 vs LUMO molecular orbitals were plotted with contour values from 0.05 to −0.05. Red and blue indicate positive and negative contributions to molecular orbitals.

no excited indole-NH_3^+ interaction. Moreover, the oscillator strength (*f*) shows the highest value at the 3^1A state for the three conformers. This 3^1A state corresponds to a wavelength in the range of 288−293 nm, which is in a good agreement with the 296 nm band obtained from magnetic circular dichroism (MCD) of 5-HT stabilized by hydrogen oxalate in 0.1 N HCl.[43]

The major MOs contributions involved in donor/acceptor exchanges concern the 1^1A and the 2^1A excited states for the three conformers and correspond respectively to HOMO/LUMO and HOMO-1/LUMO transfers. Figure 5 shows the electron cloud of these MOs distributed in each conformer and the different electron densities between two corresponding MOs. The electrons of HOMO and HOMO-1 orbitals are mainly localized within π indole ring orbitals. For LUMO, electrons are distributed to the NH_3^+ group, within a σ^* antibonding orbital. The analysis of MOs after subtraction of electron density between HOMO and LUMO, and HOMO-1 and LUMO, clearly shows that the excitation from the ground state allowed the 1^1A and 2^1A states respectively for both the **GmGp** and **GmGm** conformers. This confirms the existence of an indole/NH_3^+ through-space charge

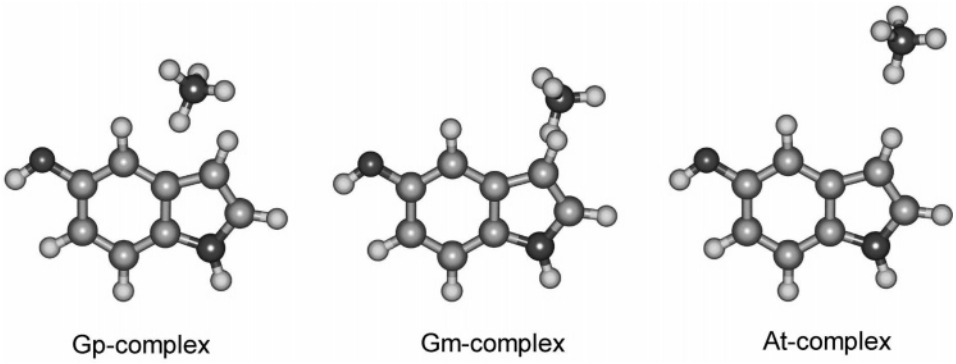

Figure 6. Structures of three NH_4^+/5-hydroxyindole complexes.

Table 4. Major Orbital Contribution, Calculated Wavelength (λ in nm), Oscillator Strength (f), and Electronic Excitation Energies (ΔE in eV) of Six Singlet-Excited States of the **GmGp**, **GmGm**, and **GmAt** Conformers of 5-HT Calculated Using the TDDFT Method at the B3LYP/6-311+G(2d,2p) Level of Theory, Together with Corresponding Ground-State Gap Energies between HOMO-n and LUMO+n (HLG in eV)

	major orbital contribution					
excited state	character	coefficients	λ (nm)	f	ΔE (eV)	HLG (eV)
			GmGp			
1^1A	HOMO→LUMO	0.69821	336.77	0.0002	3.6816	0.1590
2^1A	HOMO-1→LUMO	0.69706	309.89	0.0025	4.0009	0.1701
3^1A	HOMO→LUMO+1	0.63991	287.66	0.0725	4.3101	0.1781
			GmGm			
1^1A	HOMO→LUMO	0.70296	357.58	0.0015	3.4674	0.1485
2^1A	HOMO-1→LUMO	0.70081	318.36	0.0179	3.8945	0.1658
3^1A	HOMO→LUMO+1	0.64599	290.68	0.0874	4.2654	0.1759
			GmAt			
1^1A	HOMO→LUMO	0.70189	454.78	0.0004	2.7262	0.1183
2^1A	HOMO-1→LUMO	0.70167	402.00	0.0006	3.0842	0.1321
3^1A	HOMO→LUMO+1	0.66497	292.91	0.0777	4.2328	0.1746

transfer with a major $\pi \rightarrow$s* contribution. This is also observed by the partial electron density loss of the indole ring and their delocalization to one of the N−H bonds in the cationic head. This result again confirms the previous assignment of maximum fluorescence spectra for 5-HT at the 1^1A state. Oscillator strength of the 3^1A state of the three conformers is higher than that of the 1^1A and 2^1A states, which indicates that the low-energy absorption band in MCD of 5-HT is mainly derived from HOMO to LUMO+1 with $\pi \rightarrow$p* transfer (the plot is not shown), while this excited state is absent in the fluorescence spectra of 5-HT.

3.3. Cation-π Interactions in NH_4^+/5-Hydroxyindole Complexes. To characterize the nature and strength of the nonbonded intramolecular interactions in the 5-HT conformers, the cationic head and the 5-hydroxy indole ring of the three stable conformers **GmGm**, **GmGp**, and **GmAt** were extracted from the whole 5-HT molecule optimized geometries, and a hydrogen atom was added to the cationic head and the 5-hydroxy indole ring to fill the unsatisfied valency resulting in the suppression of the $C_{sp3}-C_{sp3}$ ethyl side chain. The resulting three complexes of NH_4^+/5-hydroxyindole named **Gp**-complex, **Gm**-complex, and **At**-complex are shown in Figure 6. For each complex we evaluated the total binding energy and its different energy term contributions. Since the results of this analysis were obtained from single point calculations, they are useful for understanding, by extrapolation, the amplitude and the nature of the intramolecular nonbonded interactions acting in the whole 5-HT molecule.

3.3.1. Intermolecular Interaction Potentials of NH_4^+/5-Hydroxyindole Complexes. Intermolecular interaction energies were calculated for the three NH_4^+/5-hydroxyindole complexes using HF and MP2 methods and the 6-311+G-(d,p) basis set. The total interaction energy and BSSE correction for the three complexes at all levels of theory are listed in Table 5. The actual interaction energies were not corrected for either zero point energy or for the thermal contribution in order to directly appreciate the correlation effect acting on the electronic energy of the nonoptimized complexes. As we can see, the binding energy is important for the three complexes and is the greatest for the **Gp**-complex, regardless of the theory level, with or without correction by the BSSE (by 3.3 and 9.6 kcal/mol with BSSE correction as compared with **Gm-** and **At-**complexes respectively). The large difference between HF and MP2 calculations for the two gauche conformers can be explained because MP2 calculations take into account the electron transitions between the occupied and the unoccupied orbitals that affect the stability of the whole 5-HT molecule. The fact that the electronic correlation effect is major for the **Gm-** and **Gp**-complexes emphasizes the important

Table 5. Absolute Binding Energies (BE) without Counterpoise Correction, Basis Set Superposition Error Correction (BSSE), and Deformation Energy (E_{def}) in kcal/mol of Three Complexes Calculated Using the HF, B3LYP, and MP2 Methods at the 6-311+(d,p) Basis Set

HF/6-311+G(d,p)			B3LYP/6-311+G(d,p)			MP2/6-311+G(d,p)		
BE	BSSE	E_{def}	BE	BSSE	E_{def}	BE	BSSE	E_{def}
				Gp				
−11.34	0.34	0.95	−14.23	0.25	0.90	−16.53	1.62	0.75
				Gm				
−8.19	0.32	0.75	−11.41	0.23	0.70	−12.98	1.38	0.58
				At				
−5.17	0.13	0.28	−6.42	0.09	0.49	−6.80	0.51	0.44

electronic redistribution occurring in the gauche conformer through a transfer of charge.

However, the relative binding energies remain quite similar when we use either the HF or the MP2 method, with or without counterpoise correction. We also observe the same tendency when we compare the relative binding energies obtained with MP2 and DFT methods. The difference between the MP2 and B3LYP results may be due to the missing long-range (1/r6) dispersion in B3LYP calculations. For each conformer, the effect of the dispersion energy is smaller than the electron correlation effects. Hence, electron correlation and dispersion energy contributions to the HF and B3LYP binding energy respectively are greater for the **Gp**- (30% and 10%) and **Gm**-complexes (40% and 10%) than for the **At** one (30% and negligible). This suggests that the position of the ammonium group of 5-HT, relative to the 5-hydroxyindole ring, is not driven by dispersion energy but rather by other energy terms. This observation was confirmed by the energy decomposition analysis.

The geometry deformation energy (E_{def}) represents the constraints imposed on the internal coordinates of the two fragments of the complexes and is calculated by the summation over the two monomers of a complex, of the energy difference between a monomer taken in the conformation it adopts inside 5-HT and after full optimization in the gas phase. As we can see in Table 5, E_{def} is negligible for the three complexes, suggesting that the deformation of the monomer geometries is modest and does not alter the relative stability of the three conformers of 5-HT brought about by nonbonded interactions. This observation suggests that, besides repulsive and attractive interactions, a strong constraint applied on the internal coordinates of the ethyl side chain of 5-HT (dihedral angles ϕ_1 and ϕ_2, opening of angles θ_1 and θ_2) could also participate in the decrease of the relative energy gap to around 1 kcal/mol between the two gauche 5-HT conformers.

Several recent studies have pointed out that the dispersion, quantified in terms of dynamical electronic correlation, provides a crucial contribution to the interaction energy between organic cations and aromatic groups and, in particular, between ammonium ions and a benzene ring.[39,44] A direct quantitative comparison of binding energies obtained from three NH_4^+/5-hydroxyindole complexes to those available for the NH_4^+/benzene complex is not possible since the indole ring of 5-HT and benzene molecule differ by their numbers of atoms and the nature of their bonds. However, we are able to compare qualitatively the geometries of the two kinds of dimers which may allow us to appreciate the importance of their dispersion energy. Lee et al. have shown that the most stable conformer for the NH_4^+/benzene complex is the one with two hydrogen atoms directed toward the benzene ring.[39b] This conformation allows an optimal through-space interaction between the benzene π−HOMO orbital and the ammonium σ^*_{N-H} LUMO antibonding orbital. If we compare the **Gp**- and **Gm**-complexes to the NH_4^+/benzene complex, only one N−H bond interacts with the five-membered ring π orbitals. Hence, the σ^*_{N-Ha} LUMO antibonding orbital and the π HOMO orbital are also tilted and cannot lead to an optimal interaction through a maximum overlap.

3.3.2. Energy Decomposition Analysis of NH_4^+/5-Hydroxyindole Complexes. To better understand the nature and weight of forces involved in the intramolecular interactions of the 5-HT conformers we analyzed the importance of individual energy components (electrostatic, polarization, charge transfer, repulsion) of the total interaction energy of NH4+/5-hydroxyindole complexes corresponding to the **GmGp**, **GmGm**, and **GmAt** conformers. The total interaction energies along with the energetic components through the KM and RVS methods using the HF theory and the 6-31G(d) and 6-311+G(d,p) basis sets are listed in Table S10 in the Supporting Information. Whatever the method used for energy decomposition, the total interaction energies (ΔE_{TOT}) and the corresponding energetic components of the **Gp**- and **Gm**-complexes are higher than those obtained for the **At**-complex at the HF/6-31G(d) level, indicating a major contribution of intermolecular interaction between the NH_4^+ and 5-hydroxy indole in gauche complexes. The largest ΔE_{TOT} is found for the **Gp**-complex. It is greater than those found for the **Gm**- and **At**-complexes by 3 and 6 kcal/mol, respectively. In the **At**-complex, the most important contribution for ΔE_{TOT} comes from the polarization effects, since ΔE_{POL} accounts for 70−80% of the total interaction energy. Clearly, there are no cation-π interactions in the **At**-complex, due to the very low charge transfer term, especially using the RVS scheme. This observation confirms the results obtained with NBO and the topological analysis of electron density. Hence, the electrostatic (ΔE_{ES}) and the exchange repulsion (ΔE_{EX}) terms, combined in the ΔE_{CEX}, have a minor contribution of around 0.5 kcal/mol.

The ΔE_{ES} and ΔE_{EX} were found to be predominant for the **Gp**- and **Gm**-complexes. The electrostatic attractive

energy in the **Gp**- and **Gm**-complexes is similar (about 0.5 kcal/mol) while ΔE_{EX}, the exchange repulsion energy, is mostly marked for the **Gm**-complex, 1.6 kcal/mol higher than that of the **Gp**-complex. The balance of these two components can be simply evaluated using the ΔE_{CEX} term, which is the summation of the ΔE_{ES} and ΔE_{EX} terms, indicating the presence of a stronger repulsion between NH_4^+ and 5-hydroxyindole in the **Gm**-complex. The polarization term (ΔE_{POL}) provides an important contribution to the total energy of the three complexes. It is important to note that the ΔE_{POL} obtained from the KM scheme appears to be overestimated, particularly for the **Gp**- (by −43.3 kcal/mol) and **Gm**-complex (no convergence found for ΔE_{POL} calculation) when the increase of basis set sets up to 6-311+G(d,p). Thus, the analysis of ΔE_{POL} is strictly considered by using the more physical RVS method. The energy decomposition analysis also reinforces the importance of charge-transfer effects (ΔE_{CT}). The stabilization due to charge transfer between the 5-hydroxyindole ring and the NH_4^+ group in the **Gp**- and **Gm**-complexes contributes for 30% and 40% (the KM method) or 20% and 30% (the RVS method) of the total interaction energy, respectively.

The above results are mainly based on the HF level with a very moderate 6-31G(d) basis set. However, the basis set dependence of the results was investigated by performing KM and RVS decomposition analysis with the 6-311+G-(d,p) basis set. As expected, the basis set superposition error (BSSE) is reduced with an enlarged basis set, in particular with the inclusion of polarization and diffusion functions. The ΔE_{ES} and ΔE_{EX} terms stay relatively constant for the **At**-complex upon extension of the basis set, while those terms change respectively by −0.35 and 1.83 kcal/mol for the **Gp**-complex and by −1.27 and 2.72 kcal/mol for the **Gm**-complex with respect to the 6-31G(d) basis set. For the RVS method, the ΔE_{POL} term increases by −1.26 and −1.16 kcal/mol for the **Gp**- and **Gm**-complexes, respectively, while a slight change (−0.43 kcal/mol) occurs for the **At**-complex. The charge-transfer energy (ΔE_{CT}) of the **Gp**-, **Gm**-, and **At**-complexes respectively decreases by 0.71, 0.65, and 0.35 kcal/mol. The total interaction energy (ΔE_{TOT}), which is the summation of all energetic terms in the RVS method, decreases by about 1 kcal/mol for gauche complexes but does not change significantly for the **At**-complex when the basis set increases from 6-31G(d) to 6-311+G(d,p).

Our results confirm that the electrostatic component (ΔE_{ES}) is significant in stabilizing cation-π interactions within the NH_4^+/5-hydroxyindole complexes. The ΔE_{ES} value is quantitatively dominant among the other components and is also the only term undergoing the highest shift when the ethylamine side chain is changed from the gauche to the anti conformation. The largest contribution to the electrostatic term is thought to be due to the interaction between the positive charge of the ammonium nitrogen and the permanent electric multipoles of the 5-hydroxyindole ring. A large number of theoretical studies, performed on several different complexes, have also shown that the cationic-π interactions are strongly governed by electrostatic interactions between a cation and the permanent quadrupole moment of an aromatic ring.[39a,45] Furthermore, the presence of an ion−dipole interaction has been proposed for a series of tetramethylammonium-aromatic complexes.[44a] Recently, the energy decomposition analysis of ammonium-π complexes with benzene, furan, pyrrole, and thiophene have shown that electrostatic interactions drive the stability of a complex formed between a positive charge centered on the ammonium nitrogen and the permanent electric multipoles of aromatic rings.[12] The authors have reported both the ion−dipole and the ion−quadrupole to significantly contribute to the electrostatic term using the KM approach.

The exchange repulsion term (ΔE_{EX}) appears to be more important in the **Gm**- than in the **Gp**-complex, both being much larger than in the **At**-complex. The increase of short-range repulsion in gauche conformers comes from the frontier orbitals overlap, which is smaller for the **At**-complex since the two monomers are far from each other. The ΔE_{EX} term also increases when we add diffusion functions on hydrogen atoms in the basis set. The polarization (ΔE_{PL}) and charge-transfer (ΔE_{CT}) terms, which contribute to cation-π interactions of the NH_4^+/5-hydroxyindole complexes are evaluated using the more accurate RVS method, which has been claimed to allow a better control over the antisymmetrization of the wave functions.[12] After ΔE_{ES}, ΔE_{PL} provides the next important contribution to the NH_4^+-5-hydroxyindole total interaction energies, which confirms the significance of the polarization effect on cation−π interactions, as noted by others.[46] The ΔE_{PL} term is assumed to mainly account from an ion-induced multipole interaction, its strength depending on the amplitude of induced multipoles in the 5-hydroxyindole ring. The charge transfer (ΔE_{CT}) between the π system and the cation fragment contributes significantly to the total interaction energy and stabilizes the NH_4^+/5-hydroxyindole complexes. This confirms the postulate of the existence of a stabilizing charge transfer in 5-HT proposed in the 1970s by Kang and Cho.[5b] This charge transfer has been precisely analyzed using the frontier orbitals theory for some ammonium−benzene complexes and indicated the existence of a through-space $\pi-\sigma^*$ charge-transfer.[39b,44g]

4. Conclusion

The present work provides a clear view on the intramolecular energy components that are driving the conformational properties of 5-HT. Our calculations show a very good agreement with experimental IR and CD spectra and also NMR data. We confirm the existence of three local minima conformers of 5-HT with OH in the anti position (**GmGp**, **GmGm**, and **GmAt**) in the gas phase, the **GmGp** and **GmGm** conformers being 5 kcal/mol more stable than the **GmAt** conformer. This higher stability for the **GmGp** and **GmGm** conformers arises from strong nonbonded interactions established between the cationic head of 5-HT and the indole ring. The previously suspected charge transfer occurring in 5-HT is confirmed by the analysis of the IR spectra. Indeed, analysis of stretch frequencies and intensities have confirmed the presence of the red-shift of the amine N−H_a stretch frequencies and elongation of the N−H_a in gauche conformers. The analysis of calculated carbon and proton shifts along with experimental data shows modifications of the strength and length of indole ring bonds upon

the influence of the cationic head. For the **GmGp** and **GmGm** conformers C_8-C_9 and C_2-C_3 bonds are elongated respectively and show a decrease in their double bond character due to a loss of electronic density in the vicinity of the bond promoted by the charge transfer. The topological analysis of charge density and natural bond orbital analyses confirms the existence of such charge transfer by revealing a bond critical point in the gauche conformers between H_a and C_3 and H_a and C_9 in the **GmGm** and **GmGp** conformers, respectively. The direction and magnitude of those charge-transfers derived from the Kohn−Sham analogue of the Fock matrix within the NBO basis shows that the charge transfers occur between the π HOMO-1 and HOMO orbitals of indole ring and the σ^*_{N-Ha} LUMO antibonding orbital. The analysis of the binding energies and their energy components in the NH_4^+/5-hydroxyindole complexes, which were generated from geometries of whole 5-HT conformers, shows that the contribution of the charge-transfer energy, although not negligible, is minor compared to other terms such as electrostatic and polarization energies.

To summarize, the two gauche conformers are stabilized by strong intramolecular nonbonded interactions. The **GmGp** and **GmGm** conformers are stabilized mainly by electrostatic interactions with a similar charge-transfer contribution. However, the higher stability of the **GmGp** over the **GmGm** conformer comes from stronger polarization and weaker exchange repulsion energy contributions. Internal coordinates energy constraints imposed on ethylamine side chain bending and dihedral angles appear to penalize the stability of the **GmGm** conformer.

To date, our work is the first to provide in detail the physical nature of the different energy contributions that influence the conformational properties of 5-HT and gives the means to interpret 5-HT experimental IR, CD, and NMR spectra. Hence, this work can be used as a solid basis for further studies such as, for example, the influence of implicit or explicit water solvent on 5-HT conformation or the chemical route leading to some physiologically active metabolites.

Acknowledgment. This study was partially supported by BioQuanta *Inside cell* Corp, CO, and the Conseil Régional de l'Ile-de-France (CRIF), grant no. 03.DAI.61F. We gratefully thank Dr. Mike Briley from NeuroBiz Consulting & Communications for the English corrections.

Supporting Information Available: Structure of 12 local minima of 5-HT (Figure S1) and their energies (in Hartrees) (Table S1) including energies of eight transition states; the values of 5-HT dihedral angles (ϕ_1, ϕ_2, and ϕ_4), all the conformers, and their relative energies (Table S2); molecular dynamics method and time evolution plots of the dihedral angles ϕ_1 and ϕ_2 during trajectory analysis (Figure S2) indicating guess transition state (Ts) of 5-HT for the QST3 calculations; geometric parameters of the three stable conformers of 5-HT: OH anti, **GmGp**, **GmGm**, **GmAt** (Table S3); predicted stretching IR spectra of the three stable conformers at the B3LYP/6-31+G(d,p) level of theory (Figure S3) and their harmonic stretching frequencies (ν) and intensities (I) (Table S4); absolute isotropic NMR shielding tensors (σ in ppm) of C and H atoms calculated using the GIAO method at the B3LYP/6-311+G(2d,2p) level of theory (Table S5); electrostatic potential derived charges of atoms in the 5-HT conformers calculated at the B3LYP/6-311+G(2d,2p) using ChelpG Scheme (Table S6); the shielding increment of amine hydrogen ($\Delta\delta$H) calculated using the GIAO method at the B3LYP/6-311+G(2d,2p) level of theory (Table S7); Fermi contact (FC), spin dipolar (SD), (paramagnetic spin−orbit PSO) contributions using the GIAO method at the B3LYP/6-311+G(2d,2p) level of theory (Table S8); electronic information of six singlet-excited states of three 5-HT conformers calculated using the TDDFT method at the B3LYP/6-311+G(2d,2p) level of theory (Table S9); and energy components of the three NH_4^+/5-hydroxyindole complexes calculated using KM and RVS energy decomposition analyses at the HF/6-31G(d) and the HF/6-311+G(d,p) levels of theory (Table S10). This material is available free of charge via the Internet at http://pubs.acs.org.

References

(1) Hoyer, D.; Hannon, J. P.; Martin, G. R. *Pharmacol. Biochem. Behav.* **2002**, *71*, 533−554.

(2) Hoyer, D.; Clarke, D. E.; Fozard, J. R.; Hartig, P. R.; Martin, G. R.; Mylecharane, E. J.; Saxena P. R.; Humphrey, P. P. *Pharmacol. Rev.* **1994**, *46*, 157−203.

(3) (a) Blakely, R. D.; De Felice, L. J.; Hartzell, H. C. *J. Exp. Biol.* **1994**, *196*, 263−281. (b) Uhl, G. R.; Johnson, P. S. *J. Exp. Biol.* **1994**, *196*, 229−236. (c) Nelson, N. *J. Neurochem.* **1998**, *71*, 1785−1803.

(4) Chattopadhyay, A.; Rukmini, R.; Mukherjee, S. *Biophys J.* **1996**, *71*, 1952−1960.

(5) (a) Courrière, P.; Coubeils, J. L.; Pullman, B. *C. R. Acad. Sci. Paris D* **1971**, *272*, 1697−1700. (b) Kang, S.; Cho, M. H. *Theor. Chim. Acta* **1971**, *22*, 176−183. (c) Kang, S.; Johnson, C. L.; Green, J. P. *Mol. Pharmacol.* **1973**, *9*, 640−648. (d) Port, G. N. J.; Pullman, B. *Theor. Chim. Acta* **1974**, *33*, 275−278.

(6) (a) Kumbar, M.; Sankar S. D. V. *J. Am. Chem. Soc.* **1975**, *97*, 7411−7416. (b) Pullman, B.; Courriere, P.; Berthod, H. *J. Med. Chem.* **1974**, *17*, 439−447.

(7) Ison, R. R.; Partington, P.; Roberts, G. C. K. *J. Pharm. Pharmacol.* **1972**, *24*, 82−85.

(8) (a) Karle, I. L.; Dragonette, K. S.; Brenner, S. A. *Acta Crystallogr.* **1965**, *19*, 713−716. (b) Thewalt, U.; Bugg, C. E. *Acta Crystallogr.* **1972**, *B28*, 82−92. (c) Amit, A.; Mester, L.; Klewe, B.; Furberg, S. *Acta Chem. Scand.* **1978**, *A32*, 267−270.

(9) Edvardsen O.; Dahl S. G. *Brain Res. Mol. Brain Res.* **1991**, *9*, 31−37.

(10) Pisterzi, L. F.; Almeida, D. R. P.; Chass, G. A.; Torday, L. L.; Papp, J. G.; Varro, A.; Csizmadia, I. G. *Chem. Phys. Lett.* **2002**, *365*, 542−551.

(11) Alagona, G.; Ghio, C.; Nagy, P. I. *J. Chem. Theory Comput.* **2005**, *1*, 801−816

(12) Aschi, M.; Mazza, F.; Nola, A. D. *J. Mol. Struct. (THEOCHEM)* **2002**, *587*, 177−188.

(13) (a) Beck, A. D. *J. Chem. Phys.* **1993**, *98*, 5648−5652. (b) Lee, C.; Yang, W.; Parr, R. G. *Phys. Rev. B* **1988**, *37*, 785−789. (c) Stevens, P. J.; Devlin, F. J.; Chabalowski, C. F.; Frisch, M. J. *J. Phys. Chem.* **1994**, *98*, 11623−11627.

(14) (a) Peng, C.; Schlegel, H. B. *Isr. J. Chem*. **1994**, *33*, 449−454. (b) Peng, C.; Ayala, P. Y.; Schlegel, H. B.; Frisch, M. J. *J. Comput. Chem.* **1996**, *17*, 49−56.

(15) (a) Brooks, B. R.; Bruccoleri, R. E.; Olafson, B. D.; States, D. J.; Swaminathan, S.; Karplus, M. *J. Comput. Chem*. **1983**, *4*, 187−212. (b) Ryckaert, J. P.; Ciccotti, G.; Berendsen, H. C. *J. Comput. Phys*. **1977**, 23, 327−341.

(16) (a) Carney, J. R.; Zwier, T. S. *J. Phys. Chem. A* **1999**, *103*, 9943−9957. (b) Dian, B. C.; Longarte, A.; Mercier, S. *J. Chem. Phys.* **2002**, *117*, 10688−10702.

(17) (a) Ditchfield, R. *Mol. Phys.* **1974**, *27*, 789−807. (b) Dodds, J. L.; McWeeny, R.; Sadlej, A. J. *Mol. Phys.* **1980**, *41*, 1419−1430. (c) Wolinski, K.; Hilton, J. F.; Pulay, P. *J. Am. Chem. Soc.* **1990**, *112*, 8251−8260.

(18) Ramsey, N. F. *Phys. Rev*. **1953**, *91*, 303−307.

(19) (a) Bader, R. F. W. *Chem. Rev*. **1991**, *91*, 893−928. (b) Cioslowski, J.; Nanayakkara, A.; Challacombe, M. *Chem. Phys. Lett.* **1993**, *203*, 137−142.

(20) (a) Reed, A. E.; Curtiss, L. A.; Weinhold, F. *Chem. Rev.* **1988**, *88*, 899−926. (b) Weinhold, F. A. *J. Mol. Struct. (THEOCHEM)* **1997**, *398*, 181−197.

(21) Gledening, E. D.; Reed, A. E.; Carpenter, J. A.; Weinhold, F. NBO Version 3.1.

(22) Runge, E.; Gross, E. K. U. *Phys. Rev. Lett.* **1984**, *52*, 997−1000.

(23) Xantheas, S. S. *J. Chem. Phys.* **1996**, *104*, 8821−8824.

(24) Boys, S. F.; Bernardi, F. *Mol. Phys.* **1970**, *19*, 553−566.

(25) Chalasinski, G.; Szczesniak, M. M. *Chem. Rev*. **2000**, *100*, 4227−4252.

(26) Kitaura, K.; Morokuma K. *Int. J. Quantum Chem*. **1976**, *10*, 325−340.

(27) Stevens, W. J.; Fink, W. H. *Chem. Phys. Lett.* **1987**, *139*, 15−22.

(28) Frisch, M. J.; Trucks, G. W.; Schlegel, H. B.; Scuseria, G. E.; Robb, M. A.; Cheeseman, J. R.; Montgomery, J. A., Jr.; Vreven, T.; Kudin, K. N.; Burant, J. C.; Millam, J. M.; Iyengar, S. S.; Tomasi, J.; Barone, V.; Mennucci, B.; Cossi, M.; Scalmani, G.; Rega, N.; Petersson, G. A.; Nakatsuji, H.; Hada, M.; Ehara, M.; Toyota, K.; Fukuda, R.; Hasegawa, J.; Ishida, M.; Nakajima, T.; Honda, Y.; Kitao, O.; Nakai, H.; Klene, M.; Li, X.; Knox, J. E.; Hratchian, H. P.; Cross, J. B.; Adamo, C.; Jaramillo, J.; Gomperts, R.; Stratmann, R. E.; Yazyev, O.; Austin, A. J.; Cammi, R.; Pomelli, C.; Ochterski, J. W.; Ayala, P. Y.; Morokuma, K.; Voth, G. A.; Salvador, P.; Dannenberg, J. J.; Zakrzewski, V. G.; Dapprich, S.; Daniels, A. D.; Strain, M. C.; Farkas, O.; Malick, D. K.; Rabuck, A. D.; Raghavachari, K.; Foresman, J. B.; Ortiz, J. V.; Cui, Q.; Baboul, A. G.; Clifford, S.; Cioslowski, J.; Stefanov, B. B.; Liu, G.; Liashenko, A.; Piskorz, P.; Komaromi, I.; Martin, R. L.; Fox, D. J.; Keith, T.; Al-Laham, M. A.; Peng, C. Y.; Nanayakkara, A.; Challacombe, M.; Gill, P. M. W.; Johnson, B.; Chen, W.; Wong, M. W.; Gonzalez, C.; Pople, J. A. *Gaussian 03, Revision A.1*; Gaussian, Inc.: Pittsburgh, PA, 2003.

(29) Chen, W.; and Gordon, M. S. *J. Phys. Chem.* **1996**, *100*, 14316−14328.

(30) Schmidt, M. W.; Baldridge, K. K.; Boatz, J. A.; Elbert, S. T.; Gordon, M. S.; Jensen, J. J.; Koseki, S.; Matsunaga, N.; Nguyen, K. A.; Su, S.; Windus, T. L.; Dupuis, M.; Montgomery, J. A. *J. Comput. Chem*. **1993**, *13*, 1347−1363.

(31) Zhurko, G. A.; Zhurko D. A.; Romanov A. Chemcrafts version 1.5 b248, a tool for visualization of quantum chemistry data (http://www.chemcraftprog.com).

(32) Bayari, S.; Die, S. *Spectrochim. Acta Part A* **2003**, *59*, 1255−1263.

(33) van Mourik T.; Emson Laura E. V. *Phys. Chem. Chem. Phys.* **2002**, *4*, 5863−5871.

(34) Barnes, A. J. *J. Mol. Struct.* **2004**, *704*, 3−9.

(35) (a) Sapper, H.; Lohmann, W. *Mol. Pharmacol.* **1976**, *12*, 605−611. (b) Kang, S. *Mol. Pharmacol.* **1979**, *16*, 1031−1039.

(36) Breneman, C. M.; Wiberg, K. B. *J. Comput. Chem.* **1990**, *11*, 361−373.

(37) Sychrovsky, V.; Grafenstein, J.; Cremer, D. *J. Chem. Phys.* **2000**, *113*, 3530−3547.

(38) (a) Bader, R. F. W. *Atoms In Molecules. A Quantum Theory*; Oxford University Press: New York, 1995. (b) Popelier, P. *Atoms In Molecules, An Introduction*; Prentice Hall: Englewood Cliffs, NJ, 2000.

(39) (a) Kim, K. S.; Tarakeshwar, P.; Lee, J. Y. *Chem. Rev.* **2000**, *100*, 4145−1486 and references therein. (b) Lee, J. Y.; Lee, S. J.; Choi, H. S.; Cho S. J.; Kim, K. S.; Ha, T.-K. *Chem. Phys. Lett.* **1995**, *232*, 67−71.

(40) Pople, J. A.; Santry, D. P. *Mol. Phys.* **1964**, *8*, 1−18.

(41) Wang, G.; Geng, L. *Anal. Chem.* **2005**, *77*, 20−29.

(42) Eftink, M. R.; Jia, Y.; Hu, D.; Ghiron, C. A. *J. Phys. Chem.* **1995**, *99*, 5713−5723.

(43) Sprinkel, F. M.; Shillady D. D.; Strickland, R. W. *J. Am. Chem. Soc*. **1975**, *97*, 6653−6657.

(44) (a) Pullman, A.; Berthier, G.; Savinelli, R. *J. Comput. Chem.* **1997**, *18*, 2012−2022. (b) Tan, X. J.; Jiang, H. L.; Zhu, W. L.; Chen K. X.; Ji, R. Y. *J. Chem. Soc., Perkin Trans. 2* **1999**, *1*, 107−112. (c) Pullman, A.; Berthier, G.; Savinelli, R. *J. Am. Chem. Soc*. **1998**, *120*, 8553−8554. (d) Minoux, H.; Chipot, C. *J. Am. Chem. Soc*. **1999**, *121*, 10366−10372. (e) Mecozzi, S.; West Jr, A. P.; Dougherty D. A. *J. Am. Chem. Soc.* **1996**, *118*, 2307−2308. (f) Berthomieu, D.; Brenner, V.; Ohanessian, G.; Denhez, J.; Millie, P.; Audier, H. E. *J. Phys. Chem.* **1995**, *99*, 712−720. (g) Kim, S. K.; Lee, J. Y.; Ha, T. K.; Kim, D. H. *J. Am. Chem. Soc*. **1994**, *116*, 7399−7400.

(45) (a) Dougherty D. A. *Science* **1996**, *271*, 163−168. (b) Luhmer, M.; Bartik, K.; Dejaegere A.; Bovy, P.; Reisse, J. *Bull. Soc. Chim. Fr*. **1994**, *131*, 603−606. (c) Williams, J. H. *Acc. Chem. Res.* **1993**, *26*, 593−598. (d) Hobza, P.; Selzle, H. L.; Schlag, E. W. *J. Am. Chem. Soc*. **1994**, *116*, 3500−3506.

(46) (a) Caldwell, J. W.; Kollman, P. A. *J. Am. Chem. Soc*. **1995**, *117*, 4177−4178. (b) Eriksson, M. A. L.; Morgantini, P.-Y.; Kollman, P. A. *J. Phys. Chem. B* **1999**, *103*, 4474−4480. (c) Cubero, E.; Luque, F. J.; Orozco, M. *Proc. Natl. Acad. Sci. U.S.A.* **1998**, *95*, 5976−5980. (d) Cubero, E.; Orozco, M.; Luque, F. J. *J. Phys. Chem. A* **1999**, *103*, 315−321.

CT0600316